Acknowledgment

The financial support of the Robert A. Welch Foundation of Houston, Texas, is gratefully acknowledged.

Manuscript submitted May 20, 1982; revised manuscript received Oct. 18, 1982.

Any discussion of this paper will appear in a Discussion Section to be published in the December 1983 JOURNAL. All discussions for the December 1983 Discussion Section should be submitted by Aug. 1, 1983.

Publication costs of this article were assisted by Rice University.

REFERENCES

1. T. E. Teeter and P. Van Risselberghe, *J. Chem. Phys.*, **22**, 759 (1954).
2. F. H. Meller, Final Report (Phase II), Contract No. N00014-66-C0139, Office of Naval Research, Washington, DC (1968).
3. K. S. Udupa, G. S. Subramanian, and H. V. K. Udupa, *Electrochim. Acta*, **16**, 1593 (1971).
4. V. Kaiser and E. Heitz, *Ber. Bunsenges. Phys. Chem.*, **77**, 818 (1973).
5. J. Ryu, T. N. Andersen, and H. Eyring, *J. Phys. Chem.*, **76**, 3278 (1972).
6. A. V. Zakharyan, N. V. Osetrova, and Yu. B. Vasilev, *Sov. Electrochem.*, **13**, 1568 (1978).
7. P. G. Russell, N. Kovac, S. Srinivasan, and M. Steinberg, *This Journal*, **124**, 1329 (1977).
8. S. Kapusta and N. Hackerman, *J. Electroanal. Chem. Interfacial Electrochem.*, **138**, 295 (1982).
9. Yu. Ya. Gurevich, Yu. V. Pleskov, and Z. A. Rotenberg, "Photoelectrochemistry," Consultants Bureau, New York (1980).
10. "International Critical Tables," McGraw Hill, New York and London (1982).
11. S. M. Cai, C. Y. Liu, S. M. Wilhelm, and N. Hackerman, Abstract 697, p. 1115, The Electrochemical Society Extended Abstracts, Montreal, Quebec, Canada, May 9-14, 1982.
12. A. Bewick and G. P. Greener, *Tetrahedron Lett.*, **53**, 4623 (1969) **54**, 391 (1970).
13. A. V. Zakharyan, Z. A. Rotenberg, N. V. Osetrova, and Yu. B. Vasilev, *Sov. Electrochem.*, **14**, 1317 (1978).
14. Yu. V. Pleskov, Z. A. Rotenberg, V. V. Eletsky, and V. I. Lakomov, *Faraday Discuss. Chem. Soc.*, **56**, 52 (1974).
15. D. Schiffrin, *ibid.*, **56**, 75 (1974).
16. G. C. Barker, A. W. Gardner, and D. C. Sammon, *This Journal*, **113**, 1182 (1966).
17. W. Paik, T. N. Andersen, and H. Eyring, *Electrochim. Acta*, **14**, 1217 (1969).
18. S. Gordon, E. J. Hart, M. S. Matheson, J. Rabani, and K. J. Thomas, *Discuss. Faraday Soc.*, **36**, 193 (1963).
19. C. Gabrielli, "Identification of Electrochemical Processes by Frequency Response Analysis," Solartron Instrumentation Group, Irvine, CA (1980).

Polymer Films on Electrodes

XI. Electrochemical Behavior of Polymer Electrodes Produced by Incorporation of Tetrathiafulvalenium in a Polyelectrolyte (Nafion) Matrix

Timothy P. Henning* and Allen J. Bard**

Department of Chemistry, University of Texas, Austin, Texas 78712

ABSTRACT

The electrochemical behavior of the cation exchange polymer Nafion containing tetrathiafulvalenium (TTF^+) on a platinum substrate is described. The polymer electrode shows cyclic voltammetric behavior similar to that of solid films of TTF on platinum. In 1.0*M* KBr the oxidized form of the electroactive molecules in the polymer (TTF^+) forms nonstoichiometric complexes with Br^-. The peak potentials in cyclic voltammetry shift with changes in concentration of supporting electrolyte, temperature, and anion of the supporting electrolyte. Very narrow cyclic voltammetric waves are observed that result in part from attractive interactions between the electroactive molecules. The separation in peak potential of the reduction and oxidation waves is explained by formation of $TTFBr_{0.7}$ which stabilizes the oxidized form (TTF^+) and makes it harder to reduce. Peak potentials for the oxidation and reduction shift closer together as the scan rate is lowered, which is explained by a "square (reaction) scheme."

The electrochemistry of layers on electrode surfaces, both solids and polymers, has been investigated by many research groups. The cyclic voltammetric behavior of the surface-confined layers frequently deviates from the theoretical "thin film" behavior of a one-electron nernstian reaction at 25°C; *i.e.*, peak width at half-height ($\Delta E_{1/2}$) of 90.6 mV and no splitting between the anodic and cathodic peaks ($\Delta E_p = E_{pa} - E_{pc} = 0$) (1). Relatively few films show a $\Delta E_{1/2}$ significantly smaller than 90.6 mV (2). These narrow cyclic voltammetric (CV) waves were attributed to interactions among the electroactive molecules and phase formation in the layer. Large peak separations observed in cyclic voltammetry at fast scan rates (1 V/sec and larger) have been attributed to slow heterogeneous kinetics and resistance effects in the layer. Even at slow scan rates, where heterogeneous kinetics and resistance usually are not of importance, finite ΔE_p values have been observed. These have been explained by kinetic effects associated with phase formation (nucleation overpotential) (2d) and interconversion between different forms of the polymer-confined electroactive molecules with different standard potentials (3).

We recently described unusual CV behavior of a polymer electrode in which tetrathiafulvalenium ion (TTF^+) was incorporated into a layer of the perfluorinated sulfonate polymer, Nafion (NAF) (4). This polymer electrode exhibited narrow ($\Delta E_{1/2} < 20$ mV) CV waves and ΔE_p of $\sim$ 150 mV at intermediate scan rates (*e.g.*, 10 mV/sec). This is remarkably similar to the electrochemical behavior of solid films of TTF. In this paper we describe more detailed studies of the electrochemical behavior of the TTF/NAF polymer electrode, examining the effects of supporting electrolyte concentration, different supporting electrolytes, temperature, and different scan rates in cyclic voltammetry. We also obtained absorption spectra of the TTF polymer on SnO_2 transparent conducting electrodes, which yielded information about the nature of the electroactive TTF molecules in the polymer. In a related paper the behavior of solution redox species on the TTF polymer electrodes is described (5).

* Electrochemical Society Student Member.
** Electrochemical Society Active Member.
Key words: cyclic voltammetry, scan rate, chronoamperometric behavior.

Experimental

Materials.—TTF (Aldrich) was purified by several vacuum sublimations. TTFCl was synthesized by dissolving TTF in benzene and adding dropwise a benzene solution which was saturated with chlorine. The purple TTFCl precipitate was washed with ether and air dried. The supporting electrolytes were used as purchased. The 970 eq wt Nafion dissolved in ethanol was a gift from the E. I. du Pont de Nemours & Company.

Apparatus.—All electrochemical experiments employed a Princeton Applied Research (PAR) Model 175 universal programmer, Model 173 potentiostat, and Model 179 digital coulometer. Slow potential scans (< 1 mV/sec) were accomplished by introducing a voltage divider between the programmer and potentiostat. The working electrode used in all the electrochemical experiments was a Pt disk (area = 0.027 cm^2) embedded in a glass rod. A Pt mesh was used as a counterelectrode and a saturated calomel electrode (SCE) was used as a reference. Resistance compensation was used at all scan rates faster than 10 mV/sec by adjusting the amount of positive feedback just short of oscillation.

Procedure.—The electrodes were prepared by covering the Pt disk with 10 μliter of an EtOH solution of Nafion (2% by weight) and allowing the EtOH to evaporate. The dry thickness of the resulting films (typically 1 μm) was determined with a Sloan Dektak surface profile measuring system. The TTF^+ was incorporated into the Nafion film by immersing the electrode in an aqueous solution of $\sim$ 1 m*M* TTFCl for 10 min. The electrode, denoted Pt/NAF,TTF^+, turned a golden color after immersion in the TTF^+ solution, indicating the incorporation of TTF^+. The average concentration of electroactive TTF in the electrode was typically about 0.3*M* as determined by the integrated charge under a steady-state CV wave.

Results

Cyclic voltammetry.—The behavior of a freshly formed Pt/NAF,TTF^+ electrode in aqueous 1.0*M* KBr is shown in Fig. 1. The first reduction scan of the electrode to TTF produced a broad cathodic wave. The oxidation of the electrode back to TTF^+ produced a sharp anodic wave which shifted toward less positive potentials with further cycling. The second reduction scan produced a sharp cathodic wave; this wave shifted very little in potential with further cycling. The Pt/NAF, TTF^+ electrode, which was originally golden in color, became colorless when the film was reduced in 1.0*M* KBr and then purple when the film was oxidized. After about 10 cycles the anodic wave attained a constant shape and peak potential. The integrated charge under the CV waves decreased for the first 4-5 cycles after which the integrated charge was about half that of the first reduction and then remained essentially constant. After about 2 hr the peak currents for the CV waves slowly decreased with continuous scanning and after about 12 hr the waves had disappeared.

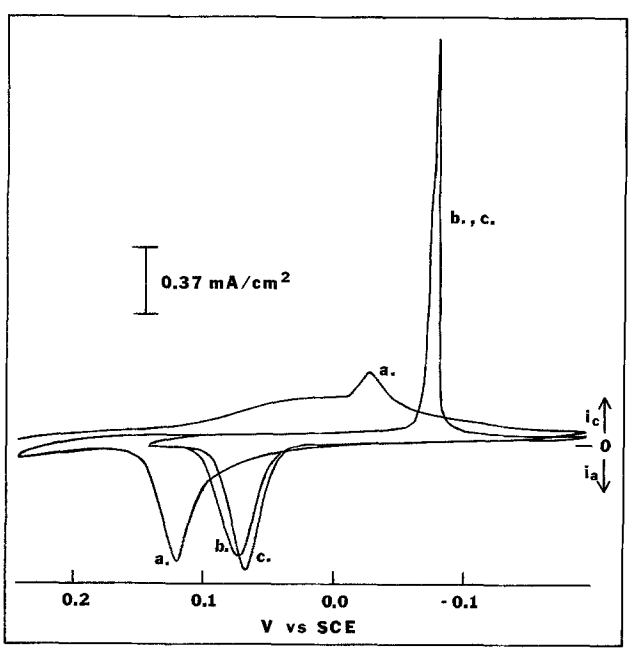

Fig. 1. Cyclic voltammogram of a Pt/NAF,TTF^+ electrode in 1*M* KBr at 10 mV/sec, (a) initial CV, first cycle; (b) third cycle; (c) fifth cycle. Integrated charge under the anodic wave, Q_t = 74 μC.

While the first CV reduction wave (Fig. 1) was a broad, drawn-out wave with a slowly decaying (diffusive) tail, which is characteristic of the CV waves seen for other electroactive molecules bound into Nafion polymer layers (6), the subsequent oxidation and reduction waves had shapes different from those previously seen in polymer electrodes. The purple color of the oxidized form of the electrode after the first and subsequent reductions has been ascribed to the formation of a $TTFBr_{0.7}$ complex, rather than the original golden material, where the TTF^+ ion is associated with the sulfonate group on the polymer. The stability of the freshly formed electrode was also very different from the electrochemically cycled electrode. When a freshly formed Pt/NAF,TTF^+ electrode was taken out of the aqueous TTFCl solution in which incorporation of TTF^+ took place, the golden-colored electrode could be immersed in water at open circuit for at least one week without any apparent effect on the subsequent electrochemistry of the polymer. If the electrode was immersed in 1.0*M* KBr, however, colored material diffused out of the polymer into the solution. Within a few minutes the amount of electroactive TTF^+ remaining in the polymer was greatly reduced over that which would have been found if the electrochemical cycling of the polymer had begun immediately. This experiment indicated that TTF^+ was indeed electrostatically bound into the Nafion polymer from the aqueous TTFCl solution and the stability of the polymer in water can be attributed to the absence of cations in solution capable of exchanging with the TTF^+ on the polymer sites. In 1.0*M* KBr, K^+ can replace TTF^+ on the polymer sites. Note, however, that after a few reduction or oxidation cycles, the electrode could be immersed at open circuit in 1*M* KBr in either the TTF^+ or TTF form with little loss of electroactive material over 1 hr. The difference in stability between the initially formed golden TTF^+ electrode and the electrochemically oxidized purple electrode in 1.0*M* KBr indicated that the electrochemically oxidized form of the polymer was very different from the initially formed material.

The steady-state cyclic voltammogram of a Pt/NAF, TTF^+ electrode is shown in Fig. 2a. For comparison, a cyclic voltammogram for a nernstian one-electron reaction showing thin layer behavior (7) with the same area under the waves is shown. This theoretical CV wave emphasizes both the unusual sharpness of the peaks and the nature of the peak separation at this scan rate. Also included in Fig. 2 is the CV of a solid film of TTF on a Pt electrode, denoted Pt/TTF. This film was formed by placing a drop of benzene containing dissolved TTF on a Pt electrode and allowing the benzene to evaporate. The similarities between the solid and polymer layers of TTF suggest that the TTF species in the polymer after cycling resembled the solid TTF and TTF^+-Br^- phases. However, while the Pt/NAF,TTF^+ electrode was reproducible and stable upon cycling for hours, the Pt/TTF electrode was less reproducible and became irreversibly oxidized in less than 1 hr of electrochemical cycling.

CV: effect of scan rate.—The CV behavior of a Pt/NAF,TTF^+ electrode was studied in 1*M* KBr for scan

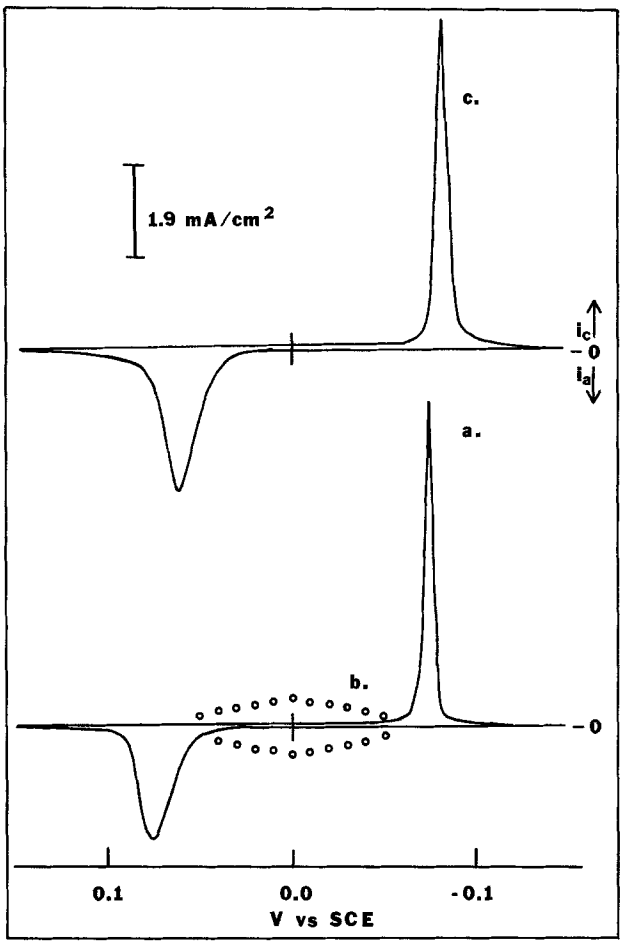

Fig. 2. Cyclic voltammogram at 10 mV/sec of (a) Pt/NAF, TTF^+ electrode in 1M KBr, $Q_t = 147\ \mu C$; (b) ideal $1e^-$ thin layer electrode using Q_t as in (a) and an $E°$ of 0.0V; (c) Pt/TTF electrode (~800Å thickness) in 1M KBr.

rates (v) of 0.02-10 V/sec (Fig. 3-5). With increasing v, the peak potential of the anodic wave (E_{pa}) shifts toward more positive values and that of the cathodic wave (E_{pc}) toward more negative values (Fig. 6). In investigations at $v < 1$ mV/sec (Fig. 3), the electrode was scanned at 1 mV/sec until ~ 150 mV before the CV wave and then v was decreased to the desired value until the peak was traversed, then increased to 1 mV/sec again until the opposite peak was reached. Although both waves shifted with increasing v, the behavior of the anodic and cathodic waves with v was

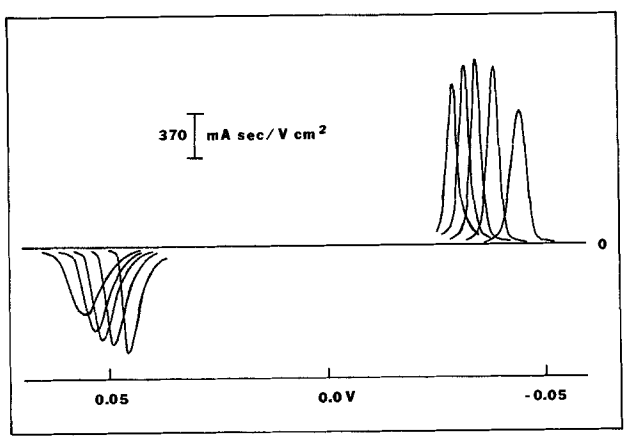

Fig. 3. Cyclic voltammogram (i_p/vA vs. E) of a Pt/NAF,TTF^+ electrode in 1M KBr at various sweep rates. The outside cathodic and anodic peaks correspond to a sweep rate of 0.5 mV/sec with subsequent anodic and cathodic peaks corresponding to sweep rates of 0.2, 0.1, 0.05, and 0.02 mV/sec. $Q_t = 152\ \mu C$.

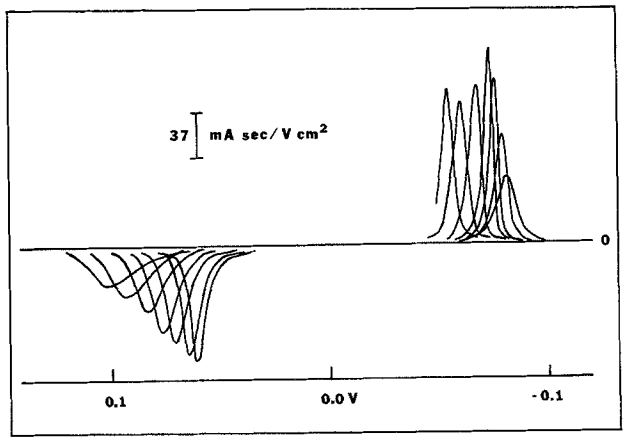

Fig. 4. Cyclic voltammogram (i_p/vA vs. E) of a Pt/NAF,TTF^+ electrode in 1M KBr at various sweep rates. The outside cathodic and anodic peaks correspond to a sweep rate of 100 mV/sec with subsequent anodic and cathodic peaks corresponding to sweep rates of 50, 20, 10, 5, 2, and 1 mV/sec. $Q_t = 44\ \mu C$.

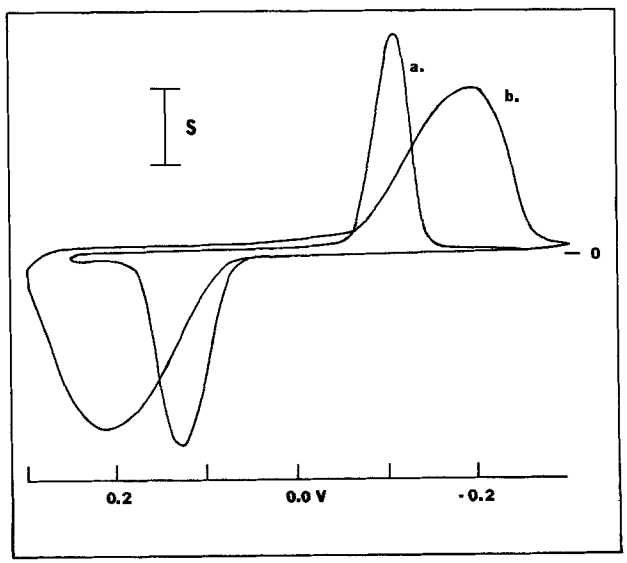

Fig. 5. Cyclic voltammogram of a Pt/NAF,TTF^+ electrode in 1M KBr at sweep rates of (a) 1 V/sec, $S = 14$ mA/cm², $Q_t = 55\ \mu C$; (b) 10 V/sec, $S = 74$ mA/cm².

different. The anodic peak shifted out and became broader and i_{pa}/v decreased with increasing v. The cathodic peak shifted out but maintained roughly the same shape, and for $v < 50$ mV/sec, i_{pc}/v was nearly the same (Fig. 4). The integrated charges under the oxidation and reduction waves were within 5% of each other and constant for the range 1-10 V/sec. The integrated charge at $v < 1$ mV/sec was not measured, but the constant shape of the waves suggests that the charge was the same for all scan rates. The electrode deteriorated more rapidly at 10 V/sec than at slower scan rates, probably because of the large current density (0.16 A/cm²) being passed through the film at this v (Fig. 5).

The shape of the CV waves of Pt/NAF,TTF^+ electrodes varied slightly from electrode to electrode; the peak currents were directly influenced by the amount of TTF^+ incorporated into the polymer layer. The examples given in the figures represent typical behavior. Because the life of any single electrode was limited, the data represent the behavior from several different electrodes. The integrated charge under a steady-state wave in cyclic voltammetry is included with each figure to make comparisons between figures easier. The CV behavior for the Pt substrate was not unique. The CV waves of the NAF-TTF polymer on Au, pyrolytic

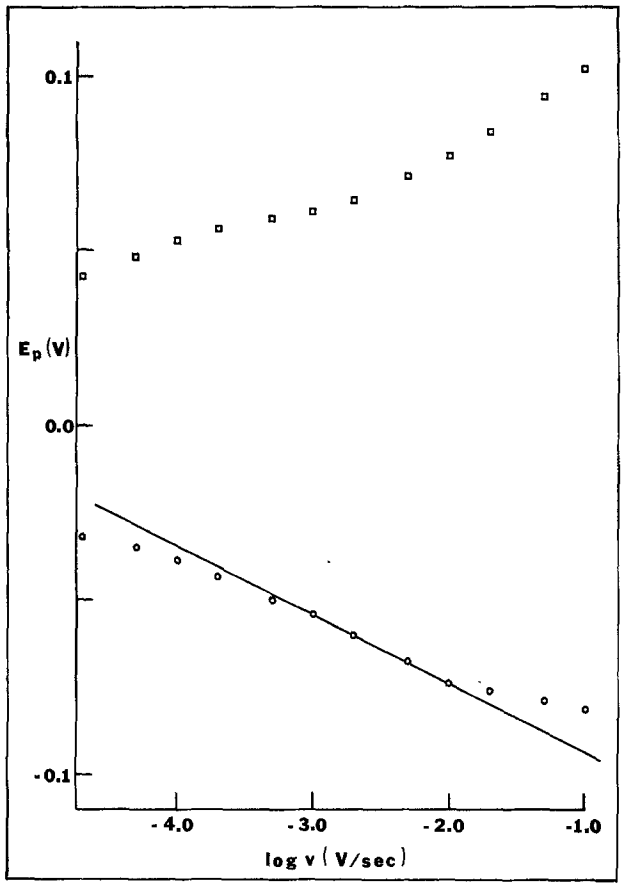

Fig. 6. Plot of E_{pc} (○) and E_{pa} (□) vs. log v. Same electrode as used in Fig. 4.

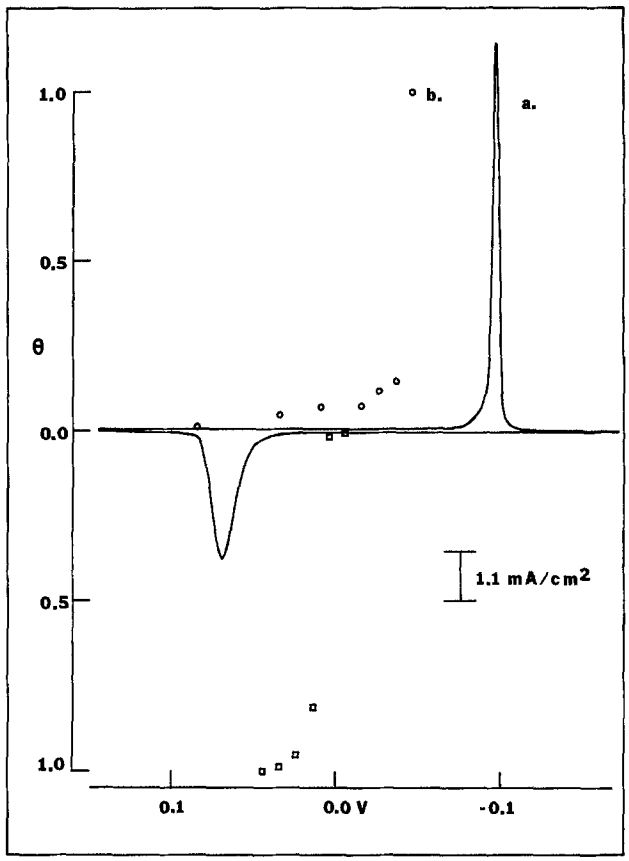

Fig. 7. (a) Cyclic voltammogram of a Pt/NAF,TTF$^+$ electrode in 1M KBr at 10 mV/sec, Q_t = 159 μC; (b) (circles and squares) electrochemical isotherm of the same electrode as shown in (a), showing total charge passed at given potential normalized to 159 μC.

graphite, optically transparent SnO_2-coated glass, and Ta substrates were very similar to that on a Pt substrate.

Equilibrium behavior.—To investigate whether the peaks would shift in and exhibit the same E_p value as equilibrium was approached, the potential was scanned to a given potential and held there until the current dropped below 1.5 nA (*i.e.*, 0.1 μC of charge per min). The ratio of the charge passed at a given potential to that needed for complete reduction or oxidation of the film, θ, as a function of E, is shown in Fig. 7. This CV isotherm taken at essentially an infinitesimal scan rate showed a sharp break in both the cathodic and anodic branches which occurred well before the peaks in the cyclic voltammogram at 10 mV/sec. If the time required for establishment of equilibrium was decreased by setting higher current limits, the effect on the isotherm was to shift the breaks in the isotherm to more negative and more positive potentials; this is the same effect as seen for the peak potentials in cyclic voltammetry with faster scan rates. The potential of the break was invariant with the amount of electroactive material reduced or oxidized in the layer during the break in the isotherm. If the potential was shifted to less negative potentials during the break in the cathodic isotherm the reaction immediately ceased. The cathodic isotherm had a long slow rise before the sharp break in the isotherm which possibly resulted from the existence of other forms of TTF$^+$, such as bound to the SO_3^- groups in the polymer.

CV: effect of scan reversal.—Reversal in the direction of a potential scan at different points along the CV wave was suggested by Conway *et al.* (8) to be a useful way of determining the effect of interactions among the molecules in the surface layer. The effect of scan reversal into both the oxidation and reduction waves of a Pt/NAF,TTF$^+$ electrode is shown in Fig. 8. The current after reversal of the scan was larger than that seen before the potential direction was reversed with this effect being more pronounced for the reduction wave. This effect is not usually seen with polymer or modified electrodes and points to strong positive (attractive) interactions among the oxidized molecules in the polymer with a smaller positive interaction among the reduced molecules. The potential of the reverse peak also showed a much larger shift for the reduction wave as compared to the oxidation wave.

CV: effect of supporting electrolyte concentration.—The concentration of supporting electrolyte was varied to determine the effect of changes in Br^- concentration on the cyclic voltammogram of a Pt/NAF,TTF$^+$ electrode. The results of varying the KBr concentration from 3.5 to 0.1*M* are shown in Fig. 9 for the same electrode. A plot of the shift in peak potential of both the cathodic and anodic waves *vs.* the log of the KBr concentrations for all concentrations investigated is shown in Fig. 10. The fact that the CV waves of the Pt/NAF,TTF$^+$ electrode responded to changes in the supporting electrolyte concentration was not surprising, because it has already been established that the oxidized form of the electrode involved formation of a TTF$^+$-Br^- complex. The shift in potential was close to the expected −59 mV per tenfold change in Br^- concentration. A significant deviation in the shape of the waves occurred at the lowest concentration, 0.1*M*. At this concentration each wave looked to be two waves, a broad diffusional looking wave with a sharper wave superimposed. Significantly, the color of the oxidized form of the wave at the lowest concentration was no longer purple but golden. The average molar concentration of electroactive TTF molecules in the polymer films, as was stated earlier, was typically 0.3*M*. The concentration of KBr present in the polymer after im-

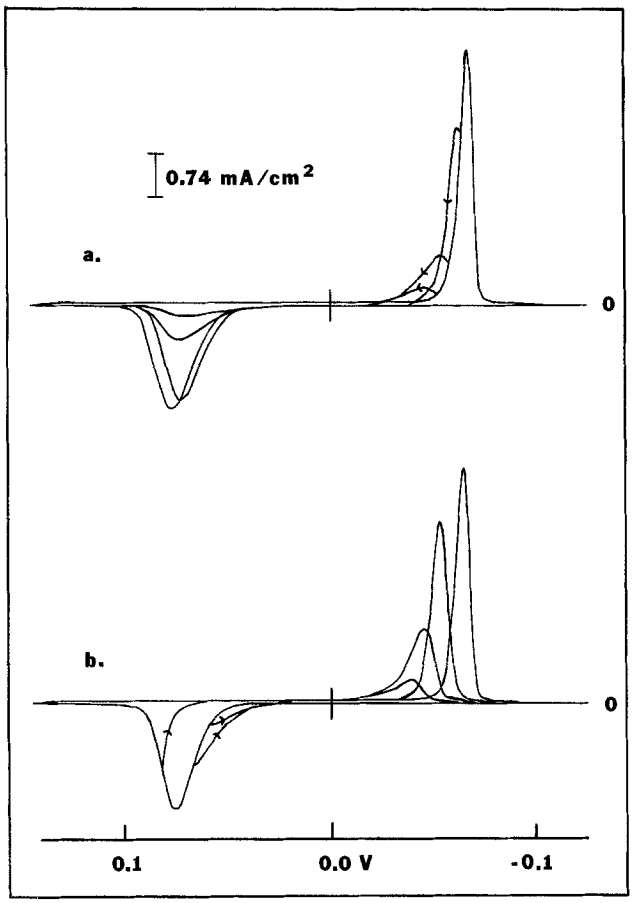

Fig. 8. Cyclic voltammogram of a Pt/NAF,TTF+ electrode in 1M KBr at 10 mV/sec with (a) scan reversal into the cathodic wave; and (b) scan reversal into the anodic wave; $Q_t = 90\ \mu C$.

mersion in a KBr solution is unknown, but examination of the polymers coated on Pt in a scanning electron microscope using energy dispersive spectroscopy showed

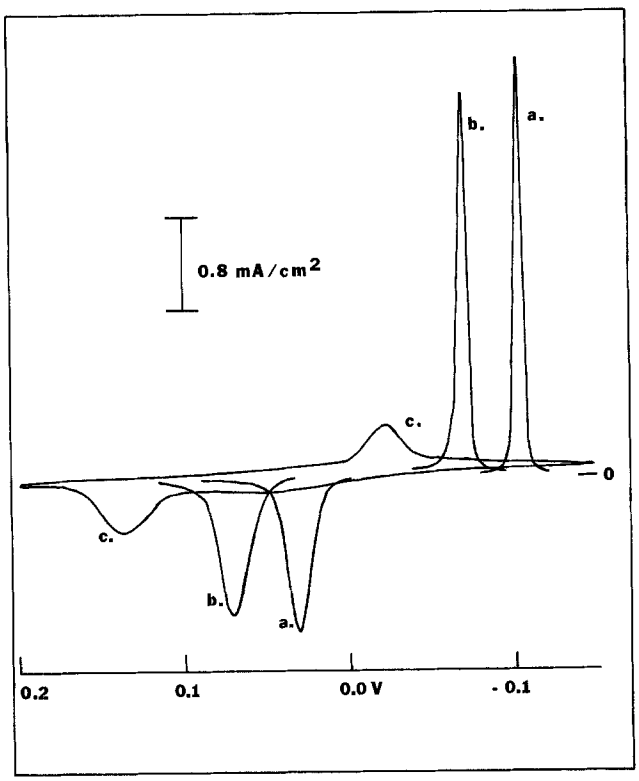

Fig. 9. Cyclic voltammogram of a Pt/NAF,TTF+ electrode at 10 mV/sec in (a) 3.48M KBr; (b) 1.0M KBr; $Q_t = 108\ \mu C$; (c) 0.1M KBr.

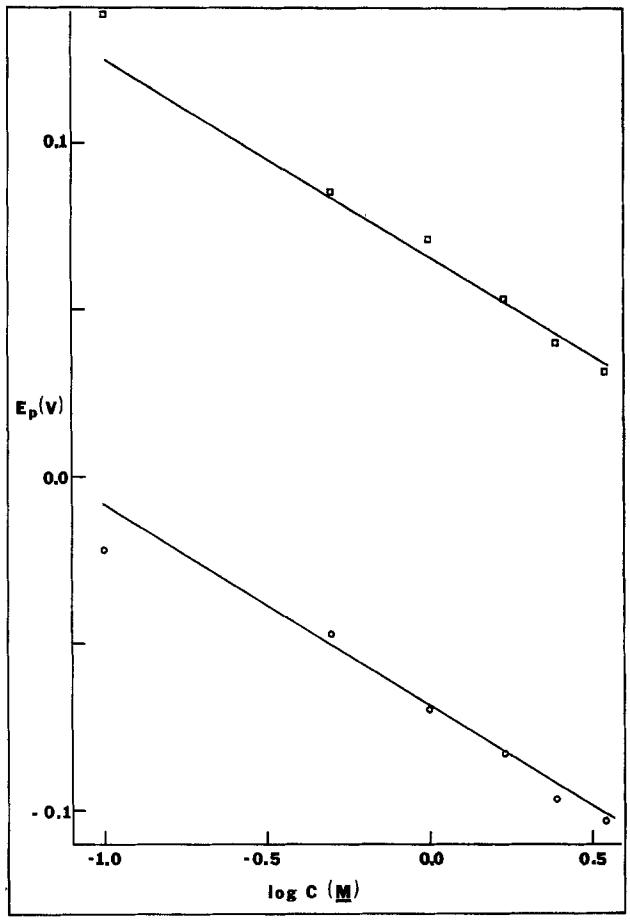

Fig. 10. Peak potential vs. log KBr concentration from the experiment shown in Fig. 9. Lines are drawn with a slope of −59 mV.

that after soaking in a KBr solution, Br was present in the polymer. Experiments using NaOH showed that after equilibration the Nafion achieved nearly the same concentration of NaOH as that present in solution (9). These facts suggested that the electrochemical process changed at the lowest concentration because of an excess in electroactive TTF over bromide ion present in the polymer.

CV: temperature effects.—The effect of varying the temperature on CV waves has been used to obtain information about the kinetics of reactions coupled to electron transfer reactions (10). Unusual temperature effects on the CV waves of TTF-TCNQ pressed pellet electrodes were previously observed (11). The temperature of the Pt/NAF,TTF+ electrode immersed in the solution was held at a given value by placing the electrochemical cell in a water bath. The SCE reference electrode remained at room temperature throughout the experiment with only the reference electrode tip in the solution. The CV waves of a Pt/NAF,TTF+ electrode were strongly temperature dependent as is shown in Fig. 11. Both the cathodic and anodic waves shifted closer together with increasing temperature. The reduction waves at the higher temperatures (36° and 55°C) were initially sharper than those at lower temperatures but within a few cycles broadened out to the shape shown in Fig. 11. The shift in peak potential with temperature was greater for the reduction wave as is shown in the plots of reduction and oxidation peak potentials *vs.* temperature (Fig. 12) which were linear over the temperature range studied.

CV: effect of different halide ions.—The halide ion in the supporting electrolyte was varied to determine the effect of the counterion on the CV waves of a Pt/NAF,TTF+ electrode (Fig. 13). The CV peaks shifted to more negative potentials in the order $Cl^- < Br^-$

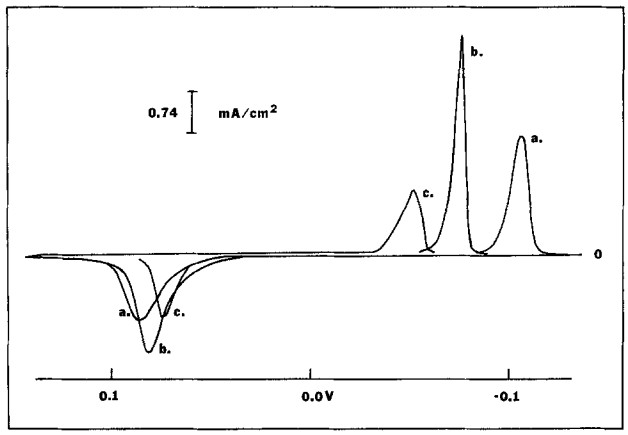

Fig. 11. Cyclic voltammogram of a Pt/NAF,TTF$^+$ electrode in 1*M* KBr at 10 mV/sec and at a temperature of (a) 1.5°C; (b) 21°C; $Q_t = 97$ μC; (c) 36°C.

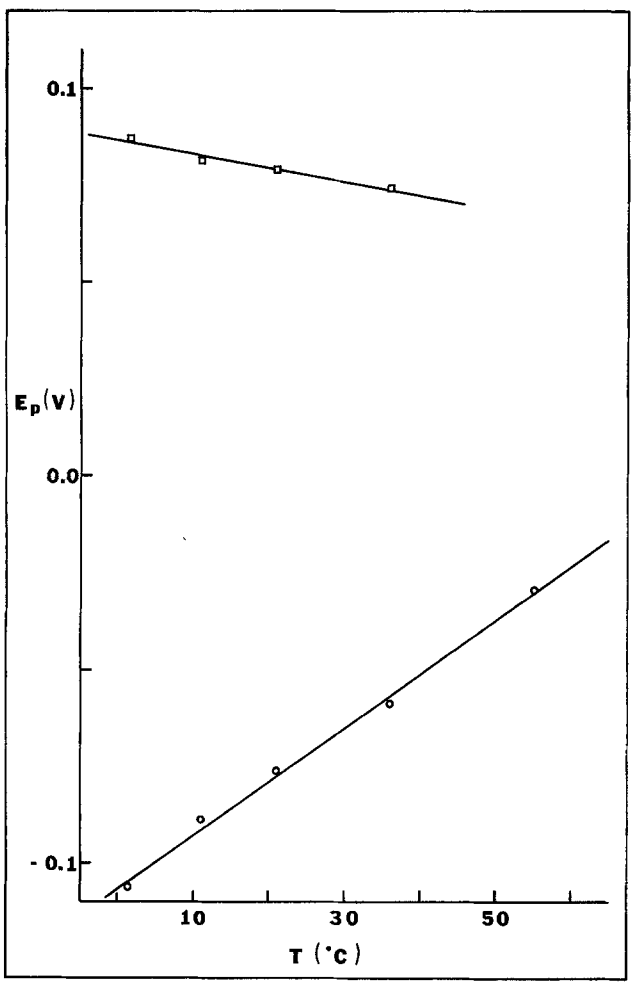

Fig. 12. Peak potential vs. temperature from the experiment shown in Fig. 11.

$< I^-$ and the oxidized form of each electrode was purple. In KF the CV waves were broad and had a shape similar to that of other electroactive molecules observed in Nafion. The shape of the CV waves and the color of the oxidized form of the electrode, golden, in KF was identical to the electrode behavior observed using potassium acetate and potassium sulfate as supporting electrolytes. TTF$^+$ is known to form one-dimensional conducting complexes with Cl^-, Br^-, and I^-, but no conducting complexes have been reported using F^-, acetate, or sulfate. If the same electrode was used in different supporting electrolytes, the behavior was unaffected by the order in which the different solutions were investigated. No effect on the cyclic voltammogram of a Pt/NAF,TTF$^+$ electrode in a Br^- solution was seen when the cation of the supporting electrolyte was changed from potassium to sodium.

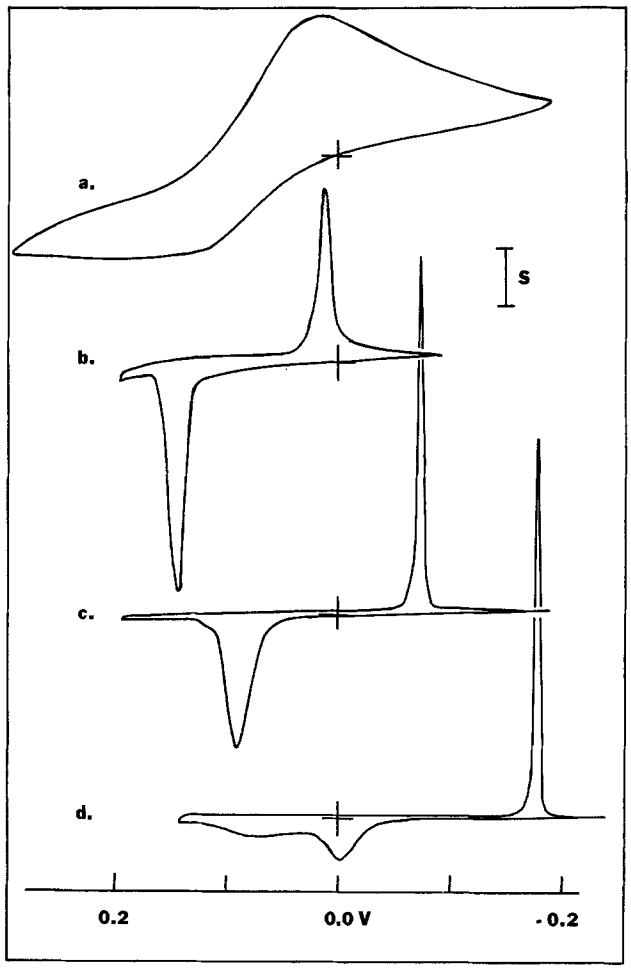

Fig. 13. Cyclic voltammogram of a Pt/NAF,TTF$^+$ electrode at 10 mV/sec in various supporting electrolytes: (a) 1*M* KF, $S = 74$ μA/cm^2; (b) 1*M* KCl, $S = 740$—(>40) μA/cm^2; (c) 1*M* KBr, $S = 740$ μA/cm^2, $Q_t = 137$ μC; (d) 1*M* KI, $S = 740$ μA/cm^2.

Chronoamperometric behavior.—Chronoamperometric methods can be useful in determining the apparent diffusion coefficient, D_{app}, of a species confined to a layer on an electrode surface. When D_{app} is measured using chronoamperometric methods, the value may be associated with a specific ion diffusion through the polymer, an electron hopping process, or both, depending on what process limits the current (12). A potential step (0-0.25V) was applied to a reduced Pt/NAF, TTF$^+$ electrode in a 1*M* KBr solution and the current-time (i-t) transient recorded. The plot of i *vs.* $t^{-1/2}$ (Fig. 14) shows a linear region with zero intercept (Cottrell region). The slope of the linear region yielded D_{app} of 8×10^{-7} cm^2/sec based on the Cottrell equation and assuming an average concentration of the electroactive TTF molecules uniformly distributed throughout the film and a one-electron process. Based on the thickness of the layer and D_{app}, the onset of deviations from Cottrell behavior which occur at longer times due to thin layer effects occurred at approximately the expected time. The current from the i-t trace for the reduction of the electrode using a potential step from 0.2 to −0.4V decayed rapidly after 2 msec, presumably showing the effect of reduction of the bulk of the TTF$^+$. The processes by which the electrode reduced and oxidized during a potential step were clearly different.

Spectroscopy.—Electrodes were formed on a transparent SnO_2 glass conducting substrate so that ab-

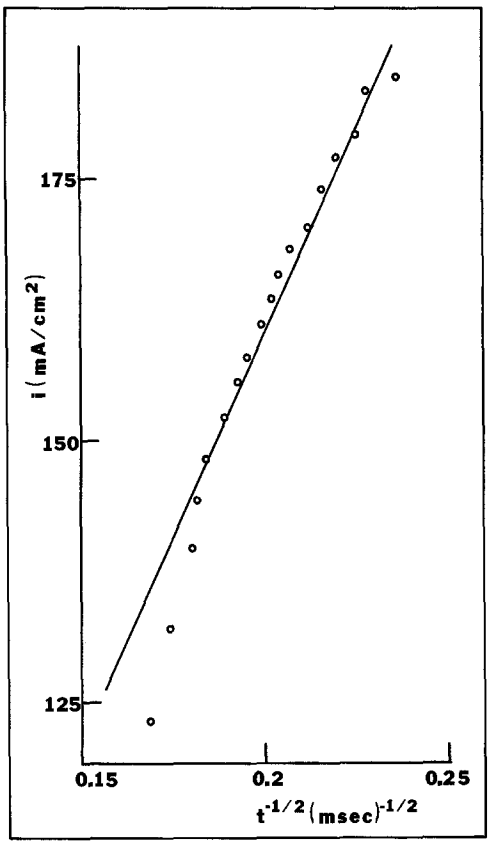

Fig. 14. Current vs. $t^{-1/2}$ for the oxidation of a Pt/NAF,TTF$^+$ electrode in 1M KBr. The potential was stepped from 0.0 to 0.25V.

sorption spectroscopy could be used to identify the form of the oxidized and reduced molecules in the polymer. The electrochemistry of the SnO_2/NAF,TTF$^+$ electrodes was similar to that of electrodes using Pt substrates. The vis-near infrared spectra of dry electrodes were recorded with a Cary 14 spectrophotometer for electrodes before electrochemical cycling and after electrochemical cycling with the electrode left in the reduced or oxidized forms (Fig. 15). The results from these spectra are shown in Table I along with results from previous studies of $TTFBr_{0.79}$ and TTFCl crystals (13). The spectrum of the electrode before electrochemical cycling was close to that of the dimer dication of TTF$^+$ as observed for TTFCl crystals (13). The peak at 790 nm (λ_{CT}) corresponds to an intermolecular electronic transition between the molecules of the dimer. The spectrum of the reduced form of the electrode did not show any peaks in the visible region; this corresponds to published spectra of TTF (13) where only an absorption peak in the u.v. was seen. The surface of the reduced form of the electrode

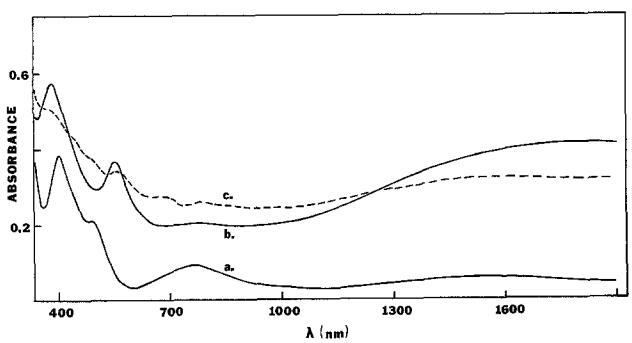

Fig. 15. Absorption spectrum of a dry glass-SnO_2/NAF,TTF$^+$ electrode (a) freshly formed; (b) after electrochemical cycling in 1M KBr, removed from solution in the oxidized state; (c) after electrochemical cycling in 1M KBr, removed from solution in the reduced state.

Table I. Absorption maxima of SnO_2/NAF,TTF$^+$ electrodes

	λ_{max} (nm)	λ_{sh} (nm)	λ_{CT} (nm)
Fresh SnO_2/NAF,TTF$^+$ electrode	400	490	760
TTFCl (dimer)*	380	530	790
Oxidized SnO_2/NAF,TTF$^+$ electrode	397	561	1890
$TTFBr_{0.79}$*	374	537	1970

* Absorption spectrum of powdered samples dispersed in KBr [from Ref. (13)].

was partially covered with the nonelectroactive crystals of $TTFBr_{0.7}$ (5), but the absence of any peaks in the spectra due to the nonelectroactive crystals means they contributed very little to the absorption spectrum. The spectrum of the electrode in the oxidized form also was similar to that for crystals of $TTFBr_{0.79}$, where the peak present in the near-infrared was shown to correspond to intermolecular electronic transitions along the conducting axis of the crystal. The presence of the near-infrared peak leads to the conclusion that the oxidized form of the electroactive molecules in the electrode was $TTFBr_{0.7\text{-}0.8}$.

Discussion

The electrochemical investigation of Pt/NAF,TTF$^+$ electrodes leads to the following model for the oxidation and reduction of the electroactive TTF molecules in the polymer layer. The consistency of the experimental results to this model is discussed below. Incorporation of TTF$^+$ into the Nafion layer produces a golden-colored film in which TTF$^+$ has no special structural arrangement and exists predominantly as TTF$^+$,$-SO_3^-$ pairs. However, upon several reduction and oxidation cycles, counterions from the electrolyte (*e.g.*, Br^- and K^+) are incorporated into the layer and the oxidized form of the layer is now purple and has an organized TTF$^+Br^-$ structure (probably in the conductive nonstoichiometric form, $TTFBr_{0.7}$). The overall redox reaction upon cycling can then be written as

$$TTFBr_{0.7} + 0.7e \rightleftharpoons TTF + 0.7Br^- \quad E^\circ_1 \qquad [1]$$

However, the structural changes that occur during these redox reactions cause the electrochemical behavior to deviate from that expected when all processes and elementary steps are rapid and reversible. Neutral TTF has a crystal structure in which the flat TTF molecules lie parallel to one another, forming stacks of TTF with each molecule assuming a staggered (st) configuration with respect to the one below it (14). The crystal structure of $TTFBr_{0.7}$ also involves stacks of TTF$^+$ molecules, but these assume an eclipsed (ec) position with respect to one another (13). The reduction of the film involves loss of Br^- and structural rearrangement of the molecules from the ec TTF$^+$ form to the st configuration of the neutral TTF molecules. The stabilization of the TTF$^+$ molecules by formation of the Br^- complex makes the complexed form of TTF$^+$ harder to reduce than the uncomplexed one. The reaction then occurs by a "square scheme" mechanism (3)

$$\begin{array}{ccc} TTFBr_{0.7}(ec) & + 0.7e - & TTF\ (ec) + 0.7Br^- \\ \uparrow k' & & \downarrow k \end{array} \qquad [2]$$

$$TTFBr_{0.7}(st) + 0.7e - \underline{TTF\ (st)} + 0.7Br^- \qquad [3]$$

(where the underlined forms are the stable ones). The E° for reaction [2] is more negative than E°_1 by an amount related to the energy difference between the ec and st forms of neutral TTF, and E° for reaction [3] is more positive than E°_1 by an amount related to the energy difference between the st and ec forms of the TTF$^+$ species. The different E°-values for oxidation and reduction result in the peak splitting shown in

the CV waves. However, the peaks do not occur at potentials governed by their respective E^{o}'s because the following irreversible reactions cause the peaks to shift in (toward E^{o}_{1}). This behavior is characteristic of reversible electron transfers followed by irreversible following reactions of solution species (an E_rC_i reaction) (1b, 15) and of surface monolayers (16). The extent of the shift in the CV peaks depends on the rate constants of the following reactions (k and k') and the scan rate (v) in a manner consistent with the behavior shown in Fig. 3 and 4. The rapidity and irreversibility of the structural rearrangements is shown by the rapid scan (v = 10 V/sec) experiments, where no reversal peaks corresponding to either reaction [2] or [3] are observed (Fig. 5). At essentially infinitesimal scan rates (Fig. 7), the behavior approaches that governed by the overall reaction, (Eq. [1]); the results suggest that $E^{o}_{1} = 0.00 \pm 0.02$V *vs.* SCE.

The model is consistent with the 59 mV shift of both peaks per tenfold change in Br^- concentration (Fig. 10). The shifts in E^{o}_{1} with supporting electrolyte anion (Fig. 13) point to stronger complexation of TTF^+ by I^- ($E^{o}_{1} \sim -0.1$V *vs.* SCE) and weaker complexation by Cl^- ($E^{o}_{1} \sim +0.05$V *vs.* SCE). Fluoride ion does not form a conductive complex, so the wave loses its thin-layer shape in a F^- medium and the structural reorganization effects are absent (Fig. 13a).

The quantitative electrochemical behavior and the detailed shapes of the waves depend on other factors, such as attractive interactions within the film which cause the extreme narrowness of the reduction peak. A digital simulation treatment of this system will be discussed elsewhere (17). However, thin layer E_rC_i behavior (16) probably is a reasonable approximation for both parts of the square scheme. The reaction of the Pt/NAF,TTF^+ electrode is considered to be thin layer at scan rates below 10 V/sec because the integrated charges under the CV waves are independent of v. The theory predicts that in the scan rate regime where the rate of the following reaction is much larger than the scan rate and the electron transfer is reversible (*i.e.*, where $(RT/n\mathbf{F})(k/v) > 10$), no peaks are observed for the unreacted form of the molecules and the variation in peak potential is described by Eq. [4] (16)

$$E_{pc} = E^{o} + (2.3RT/n\mathbf{F}) \log (RTk/n\mathbf{F}v) \qquad [4]$$

The plot of E_{pc} *vs.* log v for a Pt/NAF,TTF^+ electrode (Fig. 6) was linear over the intermediate range of scan rates ($\sim 10^{-4}$ to 10^{-2} V/sec). The slope of the line (−19.4 mV) is much smaller than that predicted by Eq. [4] for a one-electron transfer. The predicted value of $\Delta E_{1/2}$, the width at half-height, for a thin layer E_rC_i reaction is $66/n$ mV (16). The width of the anodic wave is ~20 mV but the cathodic wave is much narrower. The narrowness of the reduction wave can be explained by attractive interactions among the oxidized molecules in the polymer; these are also responsible for the unusual behavior found for scan reversal at different points into the cathodic wave, where the cathodic current increases on reversal (Fig. 8). This is explained as follows. The oxidized electrode is initially hard to reduce because the attractive interactions must be overcome; this causes the cathodic wave to be shifted to more negative potentials. As the electrode is partially reduced the retarding effect of the interactions is decreased because of the smaller concentration of oxidized molecules within the film, so the reduction rapidly accelerates, producing a narrow, tall reduction wave. This effect is less pronounced for the oxidation wave indicating that the attractive interactions among the reduced molecules are smaller than among the oxidized ones. Similarly, the $\Delta E_{1/2}$ of the oxidation wave is apparently less affected by attractive interactions than the reduction wave. If the E_rC_i model is valid for this system, the slope of the E_p *vs.* log v line suggests an n-value of 3 (*i.e.*, 3 electrons transferred per molecule). One can speculate that the critical lattice unit is $(TTF)_4Br_3$ and the overall reaction is

$$(TTF)_4Br_3 + 3e \rightleftharpoons (TTF)_4 + 3Br^- \qquad [5]$$

The deviations at high scan rates can be attributed to the onset of the significance of heterogeneous kinetics.

The effect of varying the temperature on the CV peak potentials of a Pt/NAF,TTF^+ electrode (Fig. 11) showed that the change in entropy (ΔS) for the reduction and oxidation processes were not of equal magnitude and, furthermore, did not have the same sign. This result can be explained by first assuming the cathodic and anodic processes are E_rC_i reactions in a thin layer, and then examining the temperature dependence of the peak potential for such a reaction (Eq. [4]). This is done by expressing E^{o} as a function of its enthalpic (ΔH^{o}) and entropic (ΔS^{o}) contributions and the rate constant, k, by the Arrhenius equation in terms of the activation enthalpic ($\Delta H^{\neq}$) and entropic ($\Delta S^{\neq}$) contributions. The result is Eq. [6] where h is Planck's constant and N_A is Avogadro's number. The sign is plus for a reduction and minus for an oxidation

$$n\mathbf{F}E_p = -\Delta H^{o} + T\Delta S^{o} \pm (T\Delta S^{\neq} - \Delta H^{\neq} + R \ln (RT^2/N_A n\mathbf{F}hv)) \qquad [6]$$

The derivative of Eq. [6] with respect to temperature is given by Eq. [7]

$$n\mathbf{F}\frac{dE_p}{dT} = \Delta S^{o} \pm (\Delta S^{\neq} + R \ln (R^2T^2/N_A n\mathbf{F}hv) + 2R) \qquad [7]$$

Over the experimental temperature range, dE/dT should be constant to within 2%. The experimental peaks shifted linearly with temperature (Fig. 12), with a cathodic peak slope of 1.44 mV/K, and an anodic peak slope of −0.34 mV/K. There are four terms in Eq. [7] which contribute to the slope, one of which, ΔS^{o}, has been extensively studied for solution redox species (18). The change in entropy for the reduction of a cation in solution is generally positive with dE/dT in the range 0.2-2.0 mV/K. The peak potentials of both the oxidation and reduction waves should shift to more positive potentials with increasing temperature as a result of the ΔS^{o} term. The other three terms in Eq. [7] result from the perturbation caused by the following reaction. While $\Delta S^{\neq}$ is unknown for the reaction, the other two terms can be estimated and yield ±2.79 mV/K for n = 1 (T = 298 K, v = 0.01 V/sec) and ±0.90 mV/K for n = 3 (T = 298 K, v = 0.01 V/sec) (+ for reduction, − for oxidation). The two terms cause a shift in the reduction wave to more positive potentials and the oxidation wave to more negative potentials with increasing temperature. The two calculated terms are in the same direction as the effect ΔS^{o} for the reduction peak, but are opposite to the ΔS^{o} term for the oxidation peak. This could explain why the cathodic process has a larger positive slope than the anodic process and why the anodic process has a slope with a sign opposite to that of the reduction process.

We do not believe that other explanations of the observed CV peak separations and narrow waves for Pt/NAF,TTF^+ electrodes are as reasonable. For example, resistance effects can cause peak separations in cyclic voltammetry (19), but a large resistance ($R >$ 0.1 MΩ) would be needed to cause the peak separations observed in the slow scan rate experiments, because of the small currents being passed. The cell resistance of a Pt/NAF,TTF^+ electrode in 1.0*M* KBr

was small (20Ω) as determined by observing the charging of the double layer in response to a potential step in a nonfaradaic region. A small heterogeneous electron transfer rate constant can produce peak splittings in cyclic voltammetry. However, the peak separation found at 0.02 mV/sec would yield (with $\alpha = \frac{1}{2}$ and $n_a = 1$) a rate constant, k^o, of 2×10^{-8} cm/sec (20). This seems unreasonably small compared to other values reported for electroactive molecules in Nafion (6b, c). Attractive interactions between reduced and oxidized molecules will not normally produce CV peak splittings. Large attractive interactions that occur with the onset of phase transitions can produce CV peak splittings; however, the isotherm under those conditions would not have the shape found for Pt/NAF, TTF^+ electrodes.[1]

Conclusion

A freshly formed Pt/NAF,TTF^+ electrode contains TTF^+, probably as TTF_2^{2+}, electrostatically bound on the $-SO_3^-$ cation exchange sites of the polymer. After electrochemical cycling the electroactive molecules in the polymer form small domains of solid which show similar behavior to electrodes made from thin films of TTF. This aggregation occurs within the polymer film, where the reduced form of the electroactive molecules is neutral TTF and the oxidized form is $TTFBr_{0.7}$. The sharp, narrow CV waves for the oxidation of TTF and reduction of $TFBr_{0.7}$ are split by over 100 mV; this can be explained by structural transitions between the oxidized and reduced forms. The shape and hysteresis found on scan reversal demonstrates that attractive interactions which are greater for the oxidized form exist between the electroactive molecules.

Acknowledgment

The support of this research by the National Science Foundation (CHE 7903729) and the Robert A. Welch Foundation (F-079) is gratefully acknowledged.

Manuscript submitted April 26, 1982; revised manuscript received *ca.* Sept. 14, 1982.

Any discussion of this paper will appear in a Discussion Section to be published in the December 1983 JOURNAL. All discussions for the December 1983 Discussion Section should be submitted by Aug. 1, 1983.

Publication costs of this article were assisted by the University of Texas at Austin.

[1] For a detailed discussion of peak splittings in cyclic voltammetry resulting from phase transitions, see Ref. (2d and 8).

REFERENCES

1. (a) A. J. Bard and L. R. Faulkner, "Electrochemical Methods," p. 522, John Wiley & Sons, Inc., New York (1980); (b) A. J. Bard and L. R. Faulkner, "Electrochemical Methods," Chap. 11, John Wiley & Sons, Inc., New York (1980).
2. (a) P. Daum and R. Murray, *J. Electroanal. Chem. Interfacial Electrochem.*, **103,** 289 (1979); (b) F. B. Kaufman, A. H. Schroeder, E. M. Engler, S. R. Kramer, and J. Q. Chambers, *J. Am. Chem. Soc.*, **102,** 483 (1980); (c) D. Ellis, M. Eckhoff, and V. D. Neff, *J. Phys. Chem.*, **85,** 1225 (1981); (d) A. Bewick and B. Thomas, *J. Electroanal. Chem. Interfacial Electrochem.*, **85,** 329 (1977).
3. P. Peerce and A. J. Bard, *J. Electroanal. Chem. Interfacial Electrochem.*, **114,** 89 (1980).
4. T. P. Henning, H. S. White, and A. J. Bard, *J. Am. Chem. Soc.*, **103,** 3937 (1981).
5. T. P. Henning, H. S. White, and A. J. Bard, *ibid.*, **104,** 5862 (1982).
6. (a) I. Rubinstein and A. J. Bard, *J. Am. Chem. Soc.*, **102,** 6641 (1980); (b) I. Rubinstein and A. J. Bard, *ibid.*, **103,** 5007 (1981); (c) C. Martin, I. Rubinstein, and A. J. Bard, *ibid.*, **104,** 4812 (1982).
7. A. J. Bard and L. R. Faulkner, "Electrochemical Methods," p. 410, John Wiley & Sons, Inc., New York (1980).
8. (a) E. Laviron, *J. Electroanal. Chem. Interfacial Electrochem.*, **63,** 245 (1975); (b) H. Angerstein-Kozlowaska, J. Klinger, and B. E. Conway, *ibid.*, **75,** 45 (1977); (c) E. Laviron, *ibid.*, **122,** 37 (1981).
9. T. D. Gierke, Paper 438 presented at The Electrochemical Society Meeting, Atlanta, Georgia, Oct. 9-14, 1977.
10. R. P. Van Duyne and C. N. Reilley, *Anal. Chem.*, **44,** 153 (1972).
11. C. D. Jaeger, Ph.D. Dissertation, University of Texas at Austin, 1979.
12. (a) D. A. Buttry and F. C. Anson, *J. Electroanal. Chem. Interfacial Electrochem.*, **130,** 333 (1981); (b) H. S. White, J. Leddy, and A. J. Bard, *J. Am. Chem. Soc.*, **104,** 4811 (1982).
13. J. B. Torrance, B. A. Scott, B. Welber, F. B. Kaufman, and P. E. Seiden, *Phys. Rev. B,* **19,** 730 (1979).
14. W. F. Cooper, J. W. Edwards, F. Wudl, and P. Coppers, *Cryst. Struc. Commun.*, **3,** 23 (1974).
15. R. S. Nicholson and I. Shain, *Anal. Chem.*, **36,** 706 (1964).
16. (a) E. Laviron, *J. Electroanal. Chem. Interfacial Electrochem.*, **35,** 333 (1972); (b) E. Laviron, *ibid.*, **39,** 1 (1972).
17. T. P. Henning, Ph.D. Dissertation, University of Texas at Austin, 1982.
18. E. L. Yee, R. J. Cave, K. L. Guyer, P. D. Tyma, and M. J. Weaver, *J. Am. Chem. Soc.*, **101,** 1131 (1979).
19. R. S. Nicholson, *Anal. Chem.*, **37,** 1351 (1965).
20. A. J. Bard and L. R. Faulkner, "Electrochemical Methods," p. 412, John Wiley & Sons, Inc., New York (1980).